Inorganic Chemistry

Article

pubs.acs.org/IC

Incorporation of Monovalent Cations in Sulfate Green Rust

B. C. Christiansen,[†] K. Dideriksen,[†] A. Katz,[†] S. Nedel,[†] N. Bovet,[†] H. O. Sørensen,*[,†] C. Frandsen,[‡] C. Gundlach,[‡] M. P. Andersson,[†] and S. L. S. Stipp[†]

[†]Nano-Science Center, Department of Chemistry, University of Copenhagen, Universitetsparken 5, 2100 Copenhagen, Denmark

[‡]Department of Physics, Technical University of Denmark, Fysikvej, 2800 Kongens Lyngby, Denmark

Supporting Information

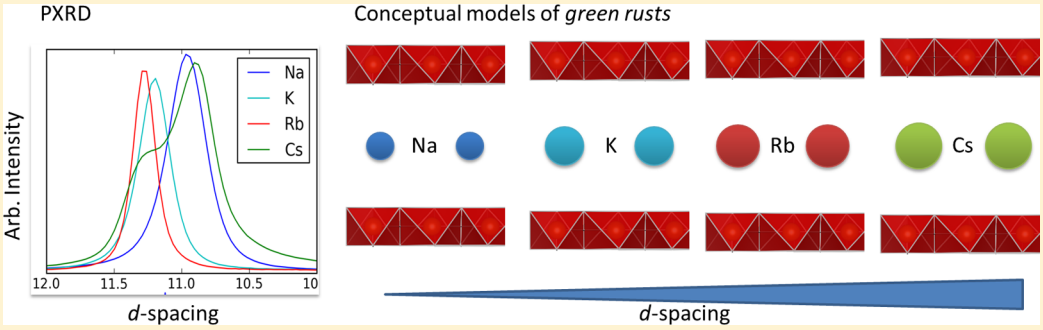

ABSTRACT: Green rust is a naturally occurring layered mixed-valent ferrous−ferric hydroxide, which can react with a range of redox-active compounds. Sulfate-bearing green rust is generally thought to have interlayers composed of sulfate and water. Here, we provide evidence that the interlayers also contain monovalent cations, using X-ray photoelectron spectroscopy and synchrotron X-ray scattering. For material synthesized with Na^+, K^+, Rb^+, or Cs^+, interlayer thickness derived from basal plane spacings correlates with the radius of the monovalent cation. In addition, sequential washing of the materials with water showed that Na^+ and K^+ were structurally fixed in the interlayer, whereas Rb^+ and Cs^+ could be removed, resulting in a decrease in the basal layer spacing. The incorporation of cations in the interlayer opens up new possibilities for the use of sulfate green rust for exchange reactions with both anions and cations: e.g., radioactive Cs.

INTRODUCTION

Green rust (GR) is a layered double hydroxide (LDH) consisting of brucite-like layers of Fe(II)−Fe(III) hydroxide with intercalated anions such as Cl^-, CO_3^{2-}, SO_3^{2-}, SO_4^{2-}, and SeO_4^{2-}.[1−5] Fe(II) in GR reacts readily with a range of redox-sensitive species. Consequently, GR oxidizes quickly in the presence of O_2, making observation of the compound difficult outside an anoxic atmosphere. GR has been reported in nature[6−8] and is known to form during corrosion of metallic Fe.[9,10] Thus, green rust's redox reactivity is likely to be important to the fate of a range of contaminants in the environment. One example is immobilization of actinides found in nuclear waste. When the mobile species TcO_4^- and NpO_2^+ react with GR, reduction occurs that leads to the formation of less soluble and mobile Tc(IV) and Np(IV).[11,12] Another example is in permeable reactive iron barriers,[13] where GR corrosion products can reduce contaminants such as chlorinated solvents, e.g. carbon tetrachloride (CCl_4),[14] tetrachloroethylene (PCE), and vinyl chloride (VC),[15] as well as heavy metals such as Cr(VI),[16,17] Hg, and Ag,[18] or act catalytically, removing Ce(III).[19]

The first structural details of GR were given by Keller,[20] Arden,[21] and Bernal et al.[4] Later, several authors[22−24] have proposed the formula to be $Fe_4^{II}Fe_2^{III}(OH)_{12}SO_4{\cdot}nH_2O$ for sulfate green rust (GR_{SO4}) on the basis of X-ray diffraction, transmission Mössbauer spectroscopy (MS), and chemical analysis. Notably, Hansen et al.[22] suggested that this formula was incomplete and that Na^+ could be part of the GR_{SO4} interlayer on the basis of the work by Drits[25] on a Na^+-incorporated Mg−Al LDH−SO_4 formed during weathering of basalt. Results from Christiansen et al.[26] showed that Na^+ from the base used during synthesis can be incorporated into the structure of GR_{SO4}. On the basis of X-ray powder diffraction (XRD), chemical analysis, and atomic force microscopy (AFM), the authors proposed the formula $Na\text{-}Fe^{II}{}_6Fe^{III}{}_3(SO_4)_2(OH)_{18}{\cdot}12H_2O$ for sodium sulfate green rust ($GR_{Na,SO4}$). Currently, it is not known if other monovalent cations can be incorporated into the GR_{SO4} interlayer or if monovalent cations are an essential part of the GR_{SO4} structure. In studies of GR_{SO4} reactivity, it is critical to understand the effect of the monovalent cations on interlayer spacing in the crystal structures of GR, because reduction of contaminants can take place in these interlayers.[27] Similarly, the presence of cations in the interlayer could influence the diffusion rate of sulfate and thus affect the redox reaction that requires exchange into the interlayer: e.g., chromate.[17] Finally, incorporation of monovalent cations is likely to affect the stability of GR_{SO4}.[28]

Received: March 3, 2014
Published: August 21, 2014

   dx.doi.org/10.1021/ic500495a | Inorg. Chem. 2014, 53, 8887−8894

The aim of this work was to determine to what extent Na^+, K^+, Rb^+, and Cs^+ can be structurally incorporated in GR_{SO4} and thereby rigorously establish if monovalent cations are part of the interlayer. GR_{SO4} was synthesized using bases containing the monovalent cations through oxidation during free drift pH, which is identical with the method previously described by Christiansen et al.[26] To characterize the crystal morphology, composition, and structure of GR_{SO4} as well as the local bonding environment of its constituents, samples were analyzed with transmission electron microscopy (TEM), X-ray photoelectron spectroscopy (XPS), synchrotron powder X-ray diffraction, pair distribution function analysis, transmission Mössbauer spectroscopy (MS), and infrared spectroscopy (IR).

MATERIALS AND METHODS

Both GR synthesis and sample preparation were carried out inside an anoxic chamber filled with 98% N_2 and 2% H_2 to avoid uncontrolled oxidation. The chamber has a PVC membrane and is equipped with palladium pellets and alumina desiccants on fan boxes to catalyze the reaction between H_2 and traces of O_2 and to remove the water produced. A gas monitor was used to follow the O_2 partial pressure (detection limit 20 ppm) and H_2 partial pressure in the chamber.

The experiments were carried out in 300 mL of perfluoroalkoxy (PFA) beakers (Savillex). Before synthesis, the PFA beakers were rinsed with doubly deionized water (Milli-Q, resistivity >18 MΩ) and soaked in a 6 M HCl solution for 24 h. The beakers were rinsed five times with Milli-Q water and allowed to air dry bottom-up. Milli-Q water used for experimental solutions was deoxygenated by bubbling N_2 (99.99%) for 2 h prior to transfer into the glovebox, where it was left for equilibration with the atmosphere for at least 4 h prior to use.

Green Rust Synthesis. GR_{SO4} was made by oxidizing an $Fe(OH)_2$ slurry with air.[26] The initial slurry was produced by dissolving 2.778 g of $FeSO_4{\cdot}7H_2O$ (Sigma Life Science, reagent grade) in 200 mL of deoxygenated, stirred ultrapure water (resistivity >18 MΩ; Milli-Q) to yield a 0.05 M Fe^{2+} solution. $Fe(OH)_2$ was precipitated by adding an aliquot of a XOH stock solution (X = Na, K, Rb, Cs) to produce an [Fe]/[OH] ratio of 0.6, which is required for synthesizing pure GR_{SO4}.[23] The base stock solution was prepared by dissolving base pellets in deoxygenated Milli-Q water inside the anoxic chamber. All hydroxides were prepared from >99% purity pellets. During synthesis, oxidation was achieved by slowly pumping CO_2-scrubbed air into the stirred (700 rpm) suspension with a peristaltic pump at 12.8 mL/min. To avoid formation of carbonate green rust, CO_2 was removed from the air by pumping it through a 20% (w/v) NaOH solution. pH (Metrohm electrode 3 M KCl) and Eh (platinum Ag/AgCl electrode in 3 M KCl) were monitored continuously during the whole reaction. When Eh and pH changes were observed, indicating a maximum concentration of GR,[26] the synthesis was stopped. However, because halting oxidation at the exact point where only GR exists is complicated, different syntheses are expected to have slightly variable abundance of accessory $Fe(OH)_2$ or Fe(III) oxides such as magnetite.

Methods. Samples of the synthesized GR_{SO4} slurry were transferred to 2 mL centrifuge tubes. To separate the solid from the solution, samples were centrifuged at 14100*g* for 5 min and the supernatant was removed. The small amount of remaining solution in contact with the solid was subsequently wicked away with the corner of a tissue. The resulting paste was either used as it was or treated with two different rinsing procedures to understand the effect on the GR structure: (i) a fast rinse to minimize the concentration of ions present in interstitial solution and adsorbed on surfaces was conducted by resuspending the solid in 2 mL of deoxygenated Milli-Q water, quickly followed by centrifugation at 14000*g* and decanting of the supernatant and (ii) a thorough rinse with Milli-Q water intended to remove labile ions from the interlayer was conducted by 3-fold, 6-fold, or 9-fold rinsing using centrifugation, rapid decanting, and resuspending. After this procedure, the solids were stored wet or dried for 48 h depending on the method for characterization.

Samples for characterization with synchrotron-based XRD were prepared by crushing the dried samples in a mortar and introducing it into a Markrörchen glass capillary tube (diameter 0.5 mm; wall thickness 0.01 mm; length 80 mm). To avoid oxidation during transport, the capillary was sealed with melted paraffin before removal from the anaerobic chamber. The XRD experiments were carried out at the beamline I811 at Max-Lab (Sweden) using an X-ray energy of 12.4 keV (λ = 1.00 Å). The data were collected piecewise, stepping a 2D Pilatus 100k detector from 3.5 to 55.5° (2θ) in 52 steps and 30 s counting time per step. A program was developed in Python to stitch the 2D images together into a 2D strip, which was azimuthally integrated to make a standard powder pattern. The program used the FabIO Python module for reading the raw data.[29] LaB_6 (ICDD PDF 34-0427) from the NIST was used as a standard for the calibration of 2θ. Magnetite,[30] observed as an impurity phase in GR, was used as an internal standard. On the basis of the magnetite Bragg reflections, a final zero shift was performed. The zero shifts were all within the uncertainty of radial resolution. The *d* spacings of the basal plane GR peaks were obtained by fitting two Gaussian functions (the Gaussian mean position was constrained to be the same for both), except for the GR synthesized with Cs^+, where four sets of two Gaussian functions were fitted to the basal peak (003).

XPS was used to measure the elemental composition of the top layers of GR. Samples were smeared as a wet paste on a sample holder made of molybdenum to produce a flat surface. The sample was transported to the instrument inside a sealed transfer chamber to minimize oxidation of GR. Prior to analysis, the GR was left to degas overnight in the XPS entry chamber, removing loosely bound water. Analysis was carried out on a Kratos AXIS Ultra^{DLD} using monochromated Al Kα (1486.6 eV) radiation (power 150 W). The analysis chamber base pressure was 5×10^{-10} mbar and it never exceeded 1×10^{-8} mbar during data collection. Wide-resolution scans were recorded with pass energies of 160 eV and high-resolution scans with 10 or 20 eV. The data were analyzed with the software casaXPS. A Shirley background was applied for quantification. Binding energies were calibrated using the adventitious C 1s peak at 285 eV.

To study the local structure of dry, rinsed, and wet $GR_{Na,SO4}$, we conducted pair distribution function (PDF) analysis of X-ray scattering data L collected at beamline 11-ID-B at the Advanced Photon Source, Argonne National Laboratory. The experiments were performed with an X-ray wavelength of 0.2128 Å. The scattering data were collected using a PerkinElmer amorphous Si 2D detector (the approximate area was 40 by 40 cm) positioned around 15 cm behind the sample. The experimental geometry was calibrated using Fit-2D[31,32] on data collected on a standard CeO_2 powder. Fit-2D was also employed for Lorentz and polarization corrections and azimuthal integration to the 1D spectrum. PDFGETX2[33,34] was subsequently used to extract PDFs. Standard corrections were applied, such as 1D background subtraction (empty or water-filled glass capillary tubes, depending on the sample medium), subtraction of the incoherent scattering, and corrections for nonlinearity in the detector response. The PDFs were acquired by Fourier transformation of the reduced total scattering structure function, $F(Q)$, using a cutoff of Q_{max} = 16 Å^{-1} to minimize the noise level in the PDFs. To determine the lattice parameters, theoretical PDFs were fitted to the experimental data using the program PDFgui.[35] Samples were prepared similarly to those for regular synchrotron powder XRD using Markrörchen glass capillary tubes with 0.9 mm diameter. Wet samples were loaded into the glass capillary with a syringe, sealed with paraffin, and centrifuged at 2000*g* using a centrifuge with a swing-out rotor. Samples were measured within 10 days of preparation.

The morphology of the particles was studied with TEM on samples prepared by resuspending a small fraction of the wet paste in 1 mL of deoxygenated Milli-Q water in a centrifuge tube. The tube was shaken to obtain a light green color and 2 μL of this solution was deposited on a carbon-covered copper grid. Finally, the sample was dried and put into a sealed box to minimize oxidation during transport to the instrument. TEM characterization was carried out on a Phillips CM20 instrument with 200 kV acceleration voltage.

dx.doi.org/10.1021/ic500495a | Inorg. Chem. 2014, 53, 8887−8894

Attenuated total reflection infrared spectroscopy (ATR-IR) measurements from 600 to 4000 cm^{-1} were conducted on material crushed using a mortar. The crushed powder was deposited on the sample holder and analyzed with a NICOLET 6700 instrument with an MCT detector. The spectral resolution was 4 cm^{-1}, and all spectra are the average of 1024 scans with a background spectrum subtracted. During the measurements, lasting less than 5 min, O_2 was not excluded. The color of the material did not change during the analysis, indicating that the extent of oxidation was minimal.

Samples for MS were prepared by mixing the unrinsed wet paste with crushed dry silica gel. The resulting dry material was pressed into thin, coin-shaped Plexiglas holders, which were sealed and stored under liquid nitrogen until measurement. Duplicate samples, from different batches of synthesis, were prepared and these were measured at low oxygen pressure at 80 K at the Technical University of Denmark using constant-acceleration spectrometers equipped with a ^{57}Co source in a rhodium matrix. The absorption lines in the spectra were fitted using Lorentzian functions. During fitting of the GR doublets, the line widths were constrained to be pairwise equal, whereas the line intensities were unconstrained in order to account for preferential orientation of the GR crystals.[36] The centroid of the spectra is given relative to that of α-Fe metal.

RESULTS AND DISCUSSION

To probe for the presence of monovalent cations in the interlayers of sulfate green rust, material was synthesized with NaOH, KOH, RbOH, or CsOH and characterized before and after rinsing with deoxygenated Milli-Q water. Figure 1 shows XPS spectra for the four types of GR studied, before and after rinsing. Even after several successive rinses, Na^+ and K^+ remained associated with the GR, with the amount of cations in the GR becoming constant after three rinses for Na and six rinses for K. In XPS, the rinsed solids displayed a cation/Fe ratio of about 0.1, consistent with the structure proposed by Christiansen et al.[26] These cations were therefore strongly associated with the solid. In contrast, only a single rinse was needed to remove all Cs^+ from GR and the Rb^+ ions were removed from the solid after three rinses. The presence of precipitated, water-soluble salts was observed by the XRD measurements for unrinsed samples only: e.g., thenardite, Na_2SO_4[37] (Supporting Information, Figure S1), and mereiterite, $K_2Fe(SO_4)_2.4H_2O$[38] (Supporting Information, Figure S2). The diffraction peaks for these sulfate minerals were not detected after rinsing the sample with Milli-Q water.

Some of the monovalent cations for the unrinsed samples stem from salts precipitated during the drying process. However, the significant XPS signals for K^+ and Na^+ remaining after extensive rinsing indicate that these cations were located in the GR crystal structure.

The XRD patterns of all GR_{SO4} samples show pronounced peaks at approximately $d \approx 11$, 5.5, and 3.7 Å (Figure 2), as expected for a green rust sulfate.[26,40,41] Bragg reflections from other phases were also observed. Peaks corresponding to magnetite (M) were observed in all of the XRD patterns and also verified by transmission electron microscopy (Supporting Information, Figure S3).

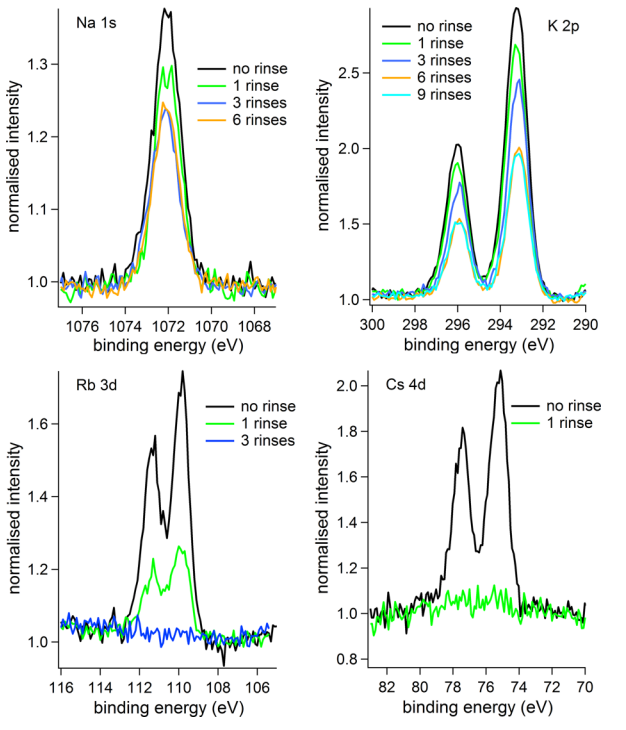

Figure 1. XPS spectra for $GR_{Na,SO4}$, $GR_{K,SO4}$, $GR_{Rb,SO4}$, and $GR_{Cs,SO4}$ after a number of rinses with deoxygenated Milli-Q water. The ability of the cation to stay associated with GR is shown. Na and K cannot be removed even after nine rinses, while three rinses are needed to remove Rb and only one rinse to make Cs disappear.

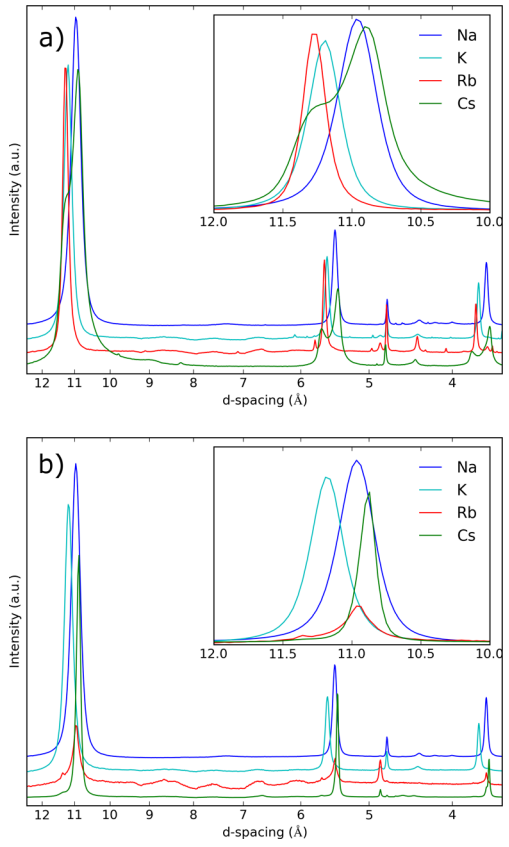

Figure 2. XRD patterns of four GR_{SO4} before (a) and after rinsing (b). (a) The strongest peaks at approximately 11, 5.5, and 3.7 Å correspond to the layered structure generally found in GR_{SO4}. The inserted zoom of the XRD spectra compares the d spacings of the 001 peaks. $GR_{Na,SO4}$ shows a peak at 10.96 Å, $GR_{K,SO4}$ at 11.20 Å, $GR_{Rb,SO4}$ at 11.28 Å, and $GR_{Cs,SO4}$ a double peak at 10.85 and 11.40 Å. (b) X-ray spectra of GR_{SO4} rinsed one time. The inserted zoom of the XRD spectra compares the d spacings of the 001 peaks. $GR_{Na,SO4}$ shows a peak at 10.96 Å, $GR_{K,SO4}$ at 11.20 Å, $GR_{Rb,SO4}$ shows a double peak at 11.23 and 10.92 Å, and $GR_{Cs,SO4}$ a peak at 10.85 Å.

dx.doi.org/10.1021/ic500495a | Inorg. Chem. 2014, 53, 8887−8894

The XRD patterns of green rust synthesized with the various monovalent cations (Figure 2) revealed small but significant differences in the positions of the Bragg reflections. The precise determination of the primary basal plane peaks (00*l*), which position depends on the interlayer thickness, allowed us to evaluate the effect of monovalent cations in the crystal structure of green rust. The (001) reflection for unrinsed $GR_{Na,SO4}$ was observed at 10.96 Å and was always unaffected by rinsing within the experimental uncertainty (2σ = 0.01 Å; Figure 2b). The 001 reflection of $GR_{K,SO4}$ (11.20 Å) was also unaffected by rinsing. This is consistent with the XPS results that showed Na^+ and K^+ in the GR structure after several rinses.

For unrinsed $GR_{Rb,SO4}$, a single sharp (001) reflection was located at 11.28 Å, but when rinsed once, XRD showed two peaks at 11.23 and 10.92 Å (Figure 2b). After 3-fold rinsing, the XRD pattern only revealed a single reflection at 10.91 Å. The XRD pattern of the unrinsed $GR_{Cs,SO4}$ featured a pronounced shoulder on the basal reflection, which was resolved by four peaks, with two main peaks at 11.40 and 10.85 Å. These match the values expected for a sample where parts of the interlayers of the crystals were filled with Cs, whereas other interlayers were cation empty. In between are a number of partially filled interlayers. After just one rinse only the reflection at 10.85 Å remained. The *d* spacing was even smaller than that of $GR_{Na,SO4}$; therefore, we consider this to be a noncation form. This is similar to what was observed in Zn−Cr−SO_4 layered double hydroxide, which collapsed to 10.9 Å when no cations were incorporated.[42] The observations of Rb and Cs correlated well with the XPS results, where the intensity of the Rb 3d peak decreased by 60% after one rinse and disappeared after three rinses. In the case of Cs, the synthesis did not produce a fully occupied interlayer. We found that the material had Cs in the interlayers, but a variation in the occupation led to wide basal plane peaks, which had to be resolved by four peaks, each consisting of two Gaussian functions with individual peak widths (Supporting Information, Figure S4). Cs was also very easy to remove from the structure, and the rinsed material actually showed a crystallite size higher than that of rinsed $GR_{Rb,SO4}$ on the basis of its peak broadening. The fact that the basal plane peaks move to a single peak at lower *d* spacings is strong proof that the cations have been incorporated in the interlayer of the GR_{SO4} structure. If that were not the case, the basal plane peaks would have been unaffected by removal of the cations.

Comparison of the full powder XRD patterns of the sodium and potassium green rust compounds shows that the compounds to a large extent are isostructural (Supporting Information, Figure S5): i.e., almost all peaks are positioned at the same *d* spacings and have similar intensities apart from the expected systematic displacement of the basal plane peaks, which is caused by a difference in cation size. Plotting of the positions of the (001) basal plane reflection and the ionic radii[39] of the cations (Figure 3) shows that these two parameters are highly correlated (R^2 = 0.997), as would be expected if the monovalent cations are dehydrated or have the same hydration shell structure in the interlayer.

An alternative to this interpretation is that the changes in basal plane *d* spacing reflect dehydration and contraction of the interlayers. Such dehydration could arise from differences in relative humidity,[43] possibly as a result of the critical relative humidity imparted by salts. For Na_2SO_4 and K_2SO_4 salts, critical relative humidity have been determined to be ∼93% and ∼98% at room temperature,[44] values that are much higher than

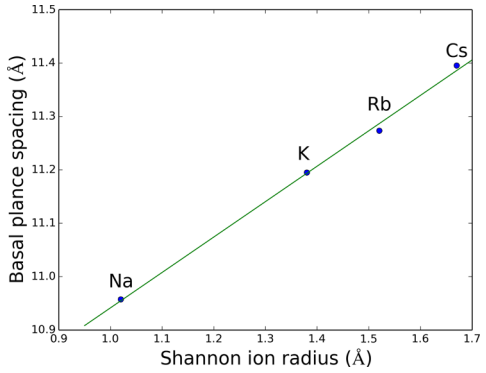

Figure 3. Correlation between basal plane *d* spacing (Å) and Shannon cation radius.[39] The line is a linear correlation with R^2 = 0.997.

those known to dehydrate GR_{SO4} (∼10% RH).[43] To probe if the smaller basal layer distance for $GR_{Na,SO4}$ is caused by dehydration, PDF analysis was carried out for dried, rinsed once, and wet material, none of which showed any peaks from Fe oxides other than GR in the raw X-ray scattering data. Figure 4 plots the obtained reduced pair distribution functions.

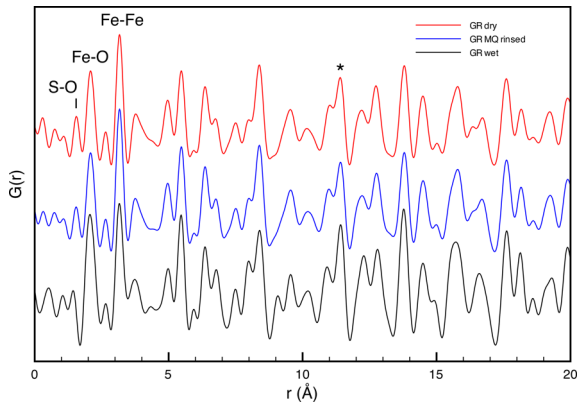

Figure 4. PDFs of dried, rinsed once, and wet $GR_{Na,SO4}$ from 0 to 20 Å. Difficulties in correcting the large background from solution result in a relatively noisy PDF for the wet material that, for example, does not clearly feature the first S−O peak at 1.55 Å. The peak labeled Fe−O represents the distance between Fe and the first neighbor O and that labeled Fe−Fe the distance between Fe and the first neighbor Fe. The peak marked with an asterisk (*) has contributions from two coordination spheres with 12 Fe atoms each, 1 within the Fe hydroxide layer and 1 across the layers.

Although the data for the wet sample are quite noisy because of difficulties in the correction of a large water background, the $GR_{Na,SO4}$ PDFs have the most peaks in common. The first major peak located at ∼2.09 Å represents the average distance between Fe and the first neighbor O in the hydroxide layers. This distance is slightly shorter than that predicted by the model of Christiansen et al.[26] The next major peak at 3.17 Å dominantly represents the average distance between Fe and the first neighbor Fe (an entity named a_0), and its value agrees well with the published model.

The PDF of the dried and the rinsed $GR_{Na,SO4}$ features a peak at ∼1.55 Å (Figure 4). The position of this peak is sensitive to variation of the maximum *Q* value used in the Fourier transform, varying from ∼1.49 Å at Q_{max} = 12 $Å^{-1}$ to ∼1.55 Å at Q_{max} = 16 $Å^{-1}$, whereas its intensity relative to the 2.09 Å peak changes only marginally. This suggests that the position is

dx.doi.org/10.1021/ic500495a | *Inorg. Chem.* 2014, 53, 8887−8894

affected by artifacts from the data reduction. Nevertheless, it presumably reflects the S−O distance of sulfate (1.49−1.51 Å).[45] This peak has decreased by 30% in the PDF of the rinsed sample, suggesting that the quick washing results in a solid somewhat poorer in sulfate, most likely because the rinsing removes sodium and sulfate that would otherwise precipitate as salts during drying.

The basal plane distance is difficult to identify directly in the PDF, because it is characterized by a Fe−Fe distance with only two Fe ions in the coordination sphere (one Fe ion in each layer above and below). The next Fe−Fe coordination sphere across the interlayer contains 12 Fe and is expected to occur at a value of 11.41 Å ($\sqrt{(c^2 + a_0^2)}$, where c is the c axis unit cell length and a_0 is the Fe−Fe distance). However, at a distance of 11.43 Å, the Fe−hydroxide layer itself has an Fe−Fe coordination sphere with a contribution of 12 Fe atoms, leading to a combined peak at 11.42 Å representing a total of 24 Fe atoms. All of the PDFs feature this peak clearly (marked with an asterisk in Figure 4), with a value of 11.40 Å for the solid sample, 11.41 Å for the 1-fold-rinsed sample, and 11.42 Å for the wet sample. These values agree excellently with those expected. The PDF of the wet sample is relatively noisy as a result of imperfect correction for the water background. This might affect the peak positions slightly. To probe the dimension of the c axis more rigorously from more peak positions, the patterns were fitted with PDFgui[35] using the structure by Christiansen et al.[26] in the r range 1.8−40 Å, which encompasses three basal planes (Supporting Information, Figure S6. The optimization routine yields c axis dimensions of 10.945 ± 0.011 Å for the dry sample, 10.945 ± 0.011 Å for the rinsed sample, and 10.957 ± 0.010 Å for the wet sample (uncertainties at 2σ). Although sodium sulfate salts could be present in dried $GR_{Na,SO4}$, the basal plane spacing does not differ measurably between the dried materials and that in solution, as would be expected if dehydration played a role. Thus, changes in basal place distance must be related to the incorporation of the monovalent cation.

MS for GR_{SO4} synthesized with Na, K, Rb, and Cs all yielded relatively similar spectra (data acquired at 80 K are shown in Figure 5). Results for duplicate (unrinsed) samples are shown. The spectra have been fitted with two doublets: (1) a doublet for Fe(II) with isomer shifts (δ) ranging from 1.26 to 1.28 mm/s and quadrupole splits (ΔE_Q) ranging from 2.84 to 2.92 mm/s at 80 K and (2) a doublet for Fe(III) with δ values of 0.44−0.46 mm/s and ΔE_Q values of 0.46−0.52 mm/s at 80 K. The area ratios between the two doublets vary from 1.6 to 2.3. The fit results are summarized in Table 1. The MS parameters are similar to those previously reported for GR_{SO4}.[40] Moreover, the variation of the parameters for duplicate material prepared with the same base is of a magnitude similar to the variation observed between samples synthesized with different bases. Thus, our MS investigation cannot unambiguously identify changes in the local structure of the Fe imparted by variation in the basal plane distance.

Infrared spectra of $GR_{Na,SO4}$, $GR_{K,SO4}$, $GR_{Rb,SO4}$, and $GR_{Cs,SO4}$ are presented in Figure 6. The vibrational bands in the region 1000−1200 cm^{-1} come from SO_4 vibrations, primarily the asymmetric stretch $\nu_3(SO_4^{2-})$, which is the only infrared-active mode for SO_4 in the tetrahedral symmetry T_d.[46] The bands are similar to those reported by Khaldi et al.[42] for a Zn−Cr LDH with Na and SO_4 (Zn−Cr−SO_4, Na). The extra peak around 1200 cm^{-1} comes from symmetry breaking and splitting of the $\nu_3(SO_4^{2-})$ vibration. It appears for Rb^+, K^+, and Na^+ and was also found by Khaldi et al.[42] for unrinsed samples, but the intensities observed for our GR_{SO4} samples are significantly lower. After 3-fold rinsing, the extra $\nu_3(SO_4^{2-})$ peak disappears (Figure 7), again similar to the observations by Khaldi et al.[42] Thenardite has an extra vibrational band for the sulfate ion at that wavelength,[47] indicating that it could represent sulfate salts. In contrast, an isolated sulfate ion with various amounts of surrounding water molecules does not show this high-frequency sulfate peak.[48] We therefore attribute the weak

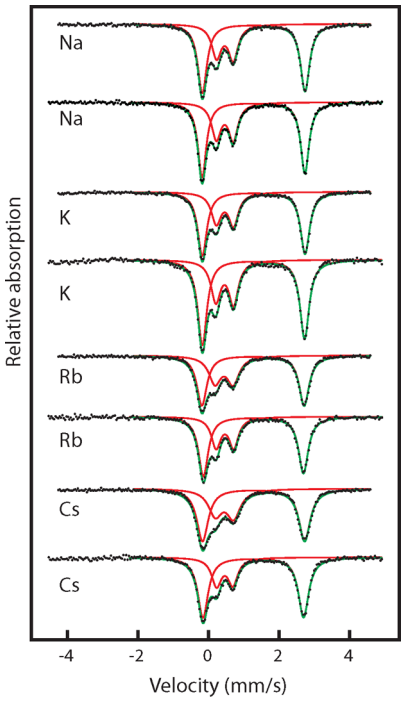

Figure 5. Mössbauer spectroscopy at 80 K for GR synthesized with different cations. The two spectra for each type of cation are measured on material from two different batches of synthesis. The black dots represent the measurements, the red lines represent the fitted individual doublets, and the green lines represent the sum of the two fitted doublets. The red and the green lines overlap in the peaks above 2 mm/s such that the red curve is not visible.

Table 1. Fitted MS Parameters for Fe(II) and Fe(III) Doublets in Green Rust Sulfate Synthesized in the Presence of Na^+, K^+, Rb^+, and Cs^+ at 80 K

GR	component	δ (mm/s)	ΔE_Q (mm/s)	line width (mm/s)	rel area (%)
Na	Fe(II)	1.28	2.91	0.31	66
	Fe(III)	0.46	0.47	0.34	34
Na	Fe(II)	1.27	2.92	0.29	64
	Fe(III)	0.46	0.48	0.33	36
K	Fe(II)	1.28	2.92	0.32	65
	Fe(III)	0.46	0.49	0.34	35
K	Fe(II)	1.27	2.90	0.32	65
	Fe(III)	0.45	0.50	0.33	35
Rb	Fe(II)	1.26	2.90	0.35	61
	Fe(III)	0.44	0.52	0.42	39
Rb	Fe(II)	1.27	2.84	0.33	67
	Fe(III)	0.46	0.50	0.32	34
Cs	Fe(II)	1.28	2.90	0.39	63
	Fe(III)	0.45	0.52	0.47	38
Cs	Fe(II)	1.27	2.85	0.36	70
	Fe(III)	0.46	0.46	0.34	30

dx.doi.org/10.1021/ic500495a | Inorg. Chem. 2014, 53, 8887−8894

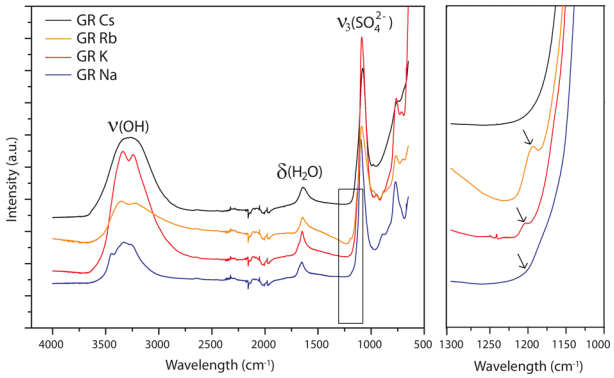

Figure 6. IR spectra for unrinsed $GR_{Na,SO4}$, $GR_{K,SO4}$, $GR_{Rb,SO4}$, and $GR_{Cs,SO4}$. The band at 3300 cm^{-1} corresponds to the stretching vibration of hydroxyl groups and water molecules. The bending vibration of water is at 1650 cm^{-1}. The vibrational band at 1100 cm^{-1} is consistent with sulfate vibrations. The small arrows show an additional weak peak at 1200 cm^{-1}, which we assign to precipitated sulfate salts.

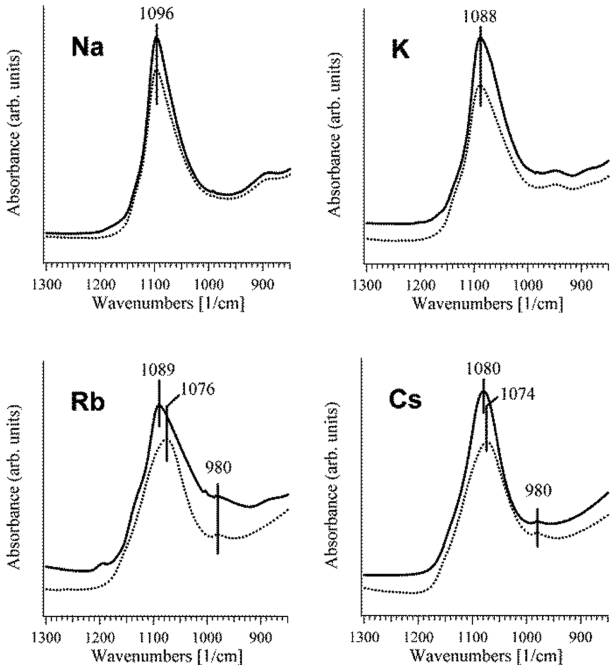

Figure 7. Comparison of IR spectra for the $\nu_3(SO_4^{2-})$ vibration for $GR_{Na,SO4}$, $GR_{K,SO4}$, $GR_{Rb,SO4}$, and $GR_{Cs,SO4}$. Solid lines denote unrinsed samples and dashed lines denote samples rinsed three times. The spectra are offset for clarity, with the rinsed samples shown below the unrinsed samples.

feature at 1200 cm^{-1} at least partially to precipitated sulfate salts, which are removed by the rinsing procedure, consistent with our X-ray scattering results.

The broad band ~3300 cm^{-1} (Figure 6) represents the stretching vibration of hydroxyl groups and water molecules. This band was split for Rb^+, K^+, and Na^+, for which XPS and XRD show that the cation is present in the structure. This band splitting is produced as a consequence of the difference in OH stretching frequencies for water molecules binding to a cation.[49] Threefold rinsing does not affect the band for K^+ and Na^+ significantly but causes the splitting to disappear for Rb^+ (Supporting Information, Figure S7), consistent with the results from XPS, which showed that three rinses remove Rb^+ completely from the solid. The splitting of the OH band at approximately 3000 cm^{-1} is more pronounced for ions in the order Na (three bands) > K (two clearly differentiated bands) > Rb (two weaker bands) > Cs (one band). This means that there is some apparent structural ordering of water that depends on the ionic radius and hydration energy for the ion. The splitting of the main OH stretching band is thus a good indicator for the presence of a hydrated cation in the interlayer of green rust. Similar OH stretch infrared band splitting was observed for hydrated Na^+ ions incorporated in CsCl.[50] The additional high-frequency peak at 3450 cm^{-1} is only present for Na and we assign it to surface hydroxyls or hydration water that is not able to act as a hydrogen bond donor in the GR structure. A water molecule or a hydroxyl group that is not acting as a hydrogen bond donor has a significantly higher OH stretching frequency.[51]

In Figure 7, we present infrared spectra of the $\nu_3(SO_4^{2-})$ vibration for rinsed and unrinsed samples. The peak position is at 1074 cm^{-1} for rinsed $GR_{Rb,SO4}$ and $GR_{Cs,SO4}$, where there are no cations in the interlayer. This value corresponds to an interlayer SO_4^{2-} ion that is not interacting with an interlayer cation. The peak positions for unrinsed $GR_{Rb,SO4}$ and rinsed and unrinsed $GR_{K,SO4}$ are shifted about 15 cm^{-1} to higher wavenumbers. The cations present in the interlayer thus interact significantly with the SO_4^{2-} ion, which breaks the intrinsic T_d symmetry and is manifested in the infrared spectrum as a peak shift. The peak position for $GR_{Na,SO4}$ at 1096 cm^{-1} is significantly higher than peak positions of the other samples, indicating an even stronger interaction with the SO_4^{2-} ion than those for Rb^+ and K^+. We have assigned the peak at 980 cm^{-1} observed for $GR_{Rb,SO4}$ and $GR_{Cs,SO4}$ (Figure 7) to the ν_1 symmetric stretch of the SO_4^{2-} ion. This band is symmetry forbidden in IR for T_d symmetry and is most clearly seen for systems where there are no cations in the structure. This suggests that when SO_4^{2-} is present in the interlayer without accompanying cations, the T_d symmetry is broken by interactions with the iron hydroxide sheets.

On the basis of the only study that determined stability constants for all the monovalent cations in question, the ease by which the cations are removed from the solid correlates with the relative stability of their aqueous sulfate ion pairs, with $NaSO_4^-$ and KSO_4^- having dissociation constants of 0.8−0.9, $RbSO_4^-$ a constant of 0.6, and $CsSO_4^-$ a constant of 0.33.[52]

CONCLUSIONS

This work shows that the monovalent cations Na^+, K^+, Rb^+, and Cs^+ incorporate in the interlayer of green rust sulfate with varying degrees of occupation. Collectively, the data show that Na^+ and K^+ are more strongly bound in the interlayer than Rb^+ and Cs^+. The observed stability of the monovalent cations in sulfate green rust correlates well with stability constants for sulfate ion pairs in aqueous solution.

The difference in the ability of incorporation and ease of rinsing shows that reactivity that involves exchange reactions would be influenced by the cation type present in the structure. Future studies should establish if there is a preference for one cation over another, similar to what is observed for anions in layered double hydroxides.[53] Thermodynamically, the presence of intercalated monovalent cations could affect GR_{SO4} stability, suggesting that additional studies are needed, similar to the one on $GR_{Na,SO4}$.[28]

dx.doi.org/10.1021/ic500495a | Inorg. Chem. 2014, 53, 8887−8894

■ ASSOCIATED CONTENT

Supporting Information

Figures showing comparisons of X-ray powder diffraction patterns for unrinsed and rinsed $GR_{Na,SO4}$ and rinsed and unrinsed $GR_{K,SO4}$, TEM images of $GR_{Na,SO4}$, $GR_{K,SO4}$, $GR_{Rb,SO4}$, and $GR_{Cs,SO4}$, background-corrected X-ray powder diffraction patterns of the 003 peak for $GR_{Cs,SO4}$, X-ray powder diffraction spectra for rinsed $GR_{Na,SO4}$ and $GR_{K,SO4}$, PDFgui fitting, and IR spectra in the OH stretch region for $GR_{Na,SO4}$, $GR_{K,SO4}$, and $GR_{Rb,SO4}$ unrinsed and rinsed three times. This material is available free of charge via the Internet at http://pubs.acs.org.

■ AUTHOR INFORMATION

Corresponding Author

*E-mail for H.O.S.: osholm@nano.ku.dk.

Notes

The authors declare no competing financial interest.

■ ACKNOWLEDGMENTS

We thank the reviewers for valuable comments. We sincerely thank Nadine Millot, who applied for an internship for A.K. at the University of Copenhagen, and are grateful for fruitful discussions with members of the NanoGeoScience group. We acknowledge MAX IV Laboratory, Lund University, for beam time at beamline i811 and Stefan Carlson for assistance. K.D. acknowledges postdoctoral funding from the Villum Kann Rasmussen Foundation and thanks Alejandro Fernandez-Martinez greatly for a thorough introduction to PDF analysis and many stimulating discussions. We are grateful for the assistance given by Karena Chapman and Kevin Beyer during PDF measurements at beamline 11-ID-B and for help in the laboratory given by Nancy Lazarz and Joanne Stubbs at GSE-CARS and by Rick Spence at beamline 11-ID-B. Financial support was granted by the Danish Councils for Independent Research (via Danscatt). C.F. acknowledges funding from the Danish Councils for Independent Research. Use of the Advanced Photon Source, an Office of Science User Facility operated for the U.S. Department of Energy (DOE) Office of Science by Argonne National Laboratory, was supported by the U.S. DOE under Contract No. DE-AC02-06CH11357. We thank Lisbeth Thygesen at the Faculty of Life, University of Copenhagen, for use of the infrared spectrometer.

■ REFERENCES

(1) Refait, P.; Abdelmoula, M.; Génin, J. M. R. *Corros. Sci.* **1998**, *40*, 1547−1560.
(2) Taylor, R. M. *Clay Miner.* **1980**, *15*, 369−382.
(3) Simon, L.; Refait, P.; Génin, J.-M. R. *Hyperfine Interact.* **1997**, *112*, 217−220.
(4) Bernal, J. D.; Dasgupta, D. R.; Mackay, A. L. *Clay Miner. Bull.* **1959**, *4*, 15−30.
(5) Refait, P.; Simon, L.; Génin, J.-M. R. *Environ. Sci. Technol.* **2000**, *34*, 819−825.
(6) Abdelmoula, M.; Trolard, F.; Bourrié, G.; Génin, J. M. R. *Hyperfine Interact.* **1998**, *112*, 235−238.
(7) Bearcock, J. M.; Perkins, W. T.; Dinelli, E.; Wade, S. C. *Mineral. Mag.* **2006**, *70*, 731−741.
(8) Christiansen, B. C.; Balic-Zunic, T.; Dideriksen, K.; Stipp, S. L. S. *Environ. Sci. Technol.* **2009**, *43*, 3436−3441.
(9) Génin, J.-M. R.; Olowe, A. A.; Resiak, B.; Confente, M.; Rollet-Benbouzid, N.; L'Haridon, S.; Prieur, D. *Hyperfine Interact.* **1994**, *93*, 1807−1812.
(10) Kounde, B.; Raharinaivo, A.; Olowe, A. A.; Rezel, D.; Bauer, P.; Génin, J.-M. R. *Hyperfine Interact.* **1989**, *46*, 421−428.
(11) Pepper, S. E.; Bunker, D. J.; Bryan, N. D.; Livens, F. R.; Charnock, J. M.; Pattrick, R. A. D.; Collison, D. *J. Colloid Interface Sci.* **2003**, *268*, 408−412.
(12) Christiansen, B. C.; Geckeis, H.; Marquardt, C. M.; Bauer, A.; Römer, J.; Wiss, T.; Schild, D.; Stipp, S. L. S. *Geochim. Cosmochim. Acta* **2011**, *75*, 1216−1226.
(13) Ritter, K.; Odziemkowski, M. S.; Gillham, R. W. *J. Contam. Hydrol.* **2002**, *55*, 87−111.
(14) Erbs, M.; Bruun Hansen, H. C.; Olsen, C. E. *Environ. Sci. Technol.* **1999**, *33*, 307−311.
(15) Lee, W.; Batchelor, B. *Environ. Sci. Technol.* **2003**, *37*, 535−541.
(16) Loyaux-Lawniczak, S.; Refait, P.; Lecomte, P.; Ehrhardt, J. J.; Génin, J. M. R. *Hydrol. Earth Syst. Sci.* **1999**, *3*, 593−599.
(17) Skovbjerg, L. L.; Stipp, S. L. S.; Utsunomiya, S.; Ewing, R. C. *Geochim. Cosmochim. Acta* **2006**, *70*, 3582−3592.
(18) O'Loughlin, E. J.; Kelly, S. D.; Kemner, K. M.; Csencsits, R.; Cook, R. E. *Chemosphere* **2003**, *53*, 437−446.
(19) Nedel, S.; Dideriksen, K.; Christiansen, B. C.; Bovet, N.; Stipp, S. L. S. *Environ. Sci. Technol.* **2010**, *44*, 4493−4498.
(20) Keller, G. Über Hydroxyde und basische Salze des 2wertigen Eisens und deren dunkelgrünen Oxydationsprodukte. Bern, Switzerland, 1948.
(21) Arden, T. V. *J. Chem. Soc.* **1950**, *1*, 882−885.
(22) Hansen, H. C. B.; Borggaard, O. K.; Sørensen, J. *Geochim. Cosmochim. Acta* **1994**, *58*, 2599−2608.
(23) Génin, J.-M. R.; Olowe, A. A.; Refait, P.; Simon, L. *Corros. Sci.* **1996**, *38*, 1751−1762.
(24) Refait, P.; Bon, C.; Simon, L.; Bourrie, G.; Trolard, F.; Bessiere, J.; Genin, J. M. R. *Clay Miner.* **1999**, *34*, 499−510.
(25) Drits, V. A.; Sokolova, T. N.; Sokolova, G. V.; Cherkashin, V. I. *Clays Clay Miner.* **1987**, *35*, 401−417.
(26) Christiansen, B. C.; Balic-Zunic, T.; Petit, P. O.; Frandsen, C.; Mørup, S.; Geckeis, H.; Katerinopoulou, A.; Stipp, S. L. S. *Geochim. Cosmochim. Acta* **2009**, *73*, 3579−3592.
(27) Bond, D. L.; Fendorf, S. *Environ. Sci. Technol.* **2003**, *37*, 2750−2757.
(28) Davesne, E.; Dideriksen, K.; Christiansen, B. C.; Sonne, M.; Ayala-Luis, K. B.; Koch, C. B.; Hansen, H. C. B.; Stipp, S. L. S. *Geochim. Cosmochim. Acta* **2010**, *74*, 6451−6467.
(29) Knudsen, E. B.; Sørensen, H. O.; Wright, J. P.; Goret, G.; Kieffer, J. *J. Appl. Crystallogr.* **2013**, *46*, 537−539.
(30) Hamilton, W. C. *Phys. Rev.* **1958**, *110*, 1050−1057.
(31) Hammersley, A. P.; Svensson, S. O.; Thompson, A. *Nucl. Instrum. Methods Phys. Res., Sect. A* **1994**, *346*, 312−321.
(32) Hammersley, A. P. *FIT2D: An Introduction and Overview*; ESRF: Grenoble, France, 1997.
(33) Chupas, P. J.; Qiu, X.; Hanson, J. C.; Lee, P. L.; Grey, C. P.; Billinge, S. J. L. *J. Appl. Crystallogr.* **2003**, *36*, 1342−1347.
(34) Qiu, X.; Thompson, J. W.; Billinge, S. J. L. *J. Appl. Crystallogr.* **2004**, *37*, 678.
(35) Farrow, C. L.; Juhas, P.; Liu, J. W.; Bryndin, D.; Božin, E. S.; Bloch, J.; Th, P.; Billinge, S. J. L. *J. Phys.: Condens. Matter* **2007**, *19*, 335219.
(36) Koch, C. B. *Hyperfine Interact.* **1998**, *117*, 131−157.
(37) Mehrotra, B. N.; Hahn, Th.; Eysel, W.; Röpke, H.; Illguth, A. *Neues Jahrb. Mineral., Monatsh.* **1978**, *9*, 408−421.
(38) Giester, G.; Rieck, B. *Eur. J. Mineral.* **1995**, *7*, 559−566.
(39) Shannon, R. D. *Acta Crystallogr., Sect. A* **1976**, *32*, 751−767.
(40) Simon, L.; François, M.; Refait, P.; Renaudin, G.; Lelaurain, M.; Génin, J.-M. R. *Solid State Sci.* **2003**, *5*, 327−334.
(41) Hansen, H. C. B., Environmental chemistry of iron(II)-iron(III) LDHs (Green Rusts). In *Layered double hydroxides: present and future*, Rives, V., Ed.; Nova Science: New York, 2001; pp 413−434.
(42) Khaldi, M.; De Roy, A.; Chaouch, M.; Besse, J. P. *J. Solid State Chem.* **1997**, *130*, 66−73.
(43) Lewis, D. G. *Adv. GeoEcol.* **1997**, *30*, 345−372.
(44) O'Brien, F. E. M. *J. Sci. Instrum. Phys. Ind.* **1948**, *25*, 73−76.
(45) Huminicki, D. M. C.; Hawthorne, F. C. *Can. Mineral.* **2003**, *41*, 79−82.

(46) Zegeye, A.; Ona-Nguema, G.; Carteret, C.; Huguet, L.; Abdelmoula, M.; Jorand, F. *Geomicrobiol. J.* **2005**, *22*, 389−399.
(47) Adler, H.; Kerr, P. F. *Am. Mineral.* **1965**, *50*, 132−147.
(48) Zhou, J.; Santambrogio, G.; Brummer, M.; Moore, D. T.; Woste, L.; Meijer, G.; Neumark, D. M.; Asmis, K. R. *J. Chem. Phys.* **2006**, *125*, 111102−5.
(49) Carnegie, P. D.; Bandyopadhyay, B.; Duncan, M. A. *J. Phys. Chem. A* **2008**, *112*, 6237−43.
(50) Yariv, S.; Shoval, S. *Appl. Spectrosc.* **1985**, *39*, 599−604.
(51) Ceponkus, J.; Uvdal, P.; Nelander, B. *J. Phys. Chem. A* **2011**, *115*, 7921−7927.
(52) Reardon, E. J. *J. Phys. Chem.* **1975**, *79*, 422−425.
(53) Miyata, S. *Clays Clay Miner.* **1983**, *31*, 305−311.